Geophysical Research Letters

RESEARCH LETTER
10.1029/2018GL079989

Key Points:
- The trend of Arctic sea ice loss accelerated after about 2000
- Decadal-time scale variability of tropical SSTs in the Pacific and Atlantic drove anomalously strong wind patterns over the Arctic after 2000
- Teleconnections from the tropics contributed to winds and ice drifts and consequent accelerated decreases of Arctic sea ice concentrations

Supporting Information:
- Supporting Information S1

Correspondence to:
G. A. Meehl,
meehl@ucar.edu

Citation:
Meehl, G. A., Chung, C. T. Y., Arblaster, J. M., Holland, M. M., & Bitz, C. M. (2018). Tropical decadal variability and the rate of Arctic sea ice decrease. *Geophysical Research Letters*, *45*, 11,326–11,333. https://doi.org/10.1029/2018GL079989

Received 19 AUG 2018
Accepted 29 SEP 2018
Accepted article online 10 OCT 2018
Published online 20 OCT 2018

Tropical Decadal Variability and the Rate of Arctic Sea Ice Decrease

Gerald A. Meehl[1], Christine T. Y. Chung[2], Julie M. Arblaster[1,3], Marika M. Holland[1], and Cecilia M. Bitz[4]

[1]National Center for Atmospheric Research, Boulder, CO, USA, [2]Bureau of Meteorology, Melbourne, Australia, [3]Australian Research Council Centre of Excellence for Climate Extremes, Monash University, Melbourne, Australia, [4]Department of Atmospheric Sciences, University of Washington, Seattle, WA, USA

Abstract The trend for cold-season (November-December-January-February, NDJF) decreases in Arctic sea ice extent from 2000 to 2014 was about a factor of two larger than the 1979–2000 trend, and the warm-season (June-July-August-September, JJAS) trend was about a factor of three larger. Sensitivity experiments with an atmospheric model show that a negative convective heating anomaly in the tropical Pacific, associated with the negative Interdecadal Pacific Oscillation phase after 2000, produces an atmospheric teleconnection pattern over the Arctic comparable to the observations in NDJF but not JJAS. A positive convective heating anomaly over the tropical Atlantic, associated with warming sea surface temperatures there in the 2000–2014 period, produces a teleconnection pattern over the Arctic comparable to the observations in JJAS but not NDJF. Thus, the observed anomalously strong Arctic surface winds and sea ice drifts after 2000, which produced accelerated decreases in sea ice extent, likely had contributions from decadal-time scale variability in the tropical Pacific and Atlantic.

Plain Language Summary Why did the trend of Arctic sea ice loss accelerate after about 2000? We show that a combination of decadally varying tropical sea surface temperatures in the Pacific and Atlantic drove seasonally dependent patterns of stronger surface winds and sea ice drifts over the Arctic that produced accelerated decreases of Arctic sea ice concentrations after 2000.

1. Introduction

Previous studies have shown connections between tropical decadal-time scale variability and high-latitude processes, including changes in sea ice. For example, the observed accelerated expansion of Antarctic sea ice from 2000 to 2014 likely had a connection to sea surface temperature (SST), precipitation, and convective heating anomalies on decadal time scales in the tropical Pacific and Atlantic (e.g., Li et al., 2014; Meehl et al., 2016; Purich, 2016, and others).

Teleconnection patterns driven by variability in the tropical oceans can produce surface wind forcing that may have also contributed to the observed changes in Arctic sea ice extent (Ding et al., 2014; Lee et al., 2011). Additionally, there is some evidence that forcing from the Arctic itself can affect teleconnections in some areas of the Northern Hemisphere (Cohen et al., 2018; Screen et al., 2018). Alternately, a two-stage set of processes has been proposed, whereby conditions in the Arctic could produce changes in the tropics, and the resulting teleconnections from those low-latitude regions could then affect conditions in the Arctic (Cvijanovic et al., 2017). Since such teleconnection patterns, which can be traced back to tropical forcing, are global, we ask the question here whether such tropical forcings, with their own decadal variability, could have contributed to the rate of sea ice loss in the Arctic in different decadal epochs.

2. Results

A time series of Arctic sea ice extent (Figure 1; concentrations are shown later for area averages and are comparable to extent) shows, for the cold season (defined here as November-December-January-February, NDJF), a trend from 2000 to 2014 of $-0.055 \cdot 10^6$ km^2 yr^{-1}. This is roughly a factor of two larger than the trend from 1979 to 1999 of $-0.031 \cdot 10^6$ km^2 yr^{-1}. Meanwhile, for the warm season (defined here as June-July-August-September, JJAS), the post-2000 trend was nearly a factor of three larger than the 1979–1999 trend ($-0.110 \cdot 10^6$ km^2 yr^{-1} post-2000, $-0.041 \cdot 10^6$ km^2 yr^{-1} pre-2000). This acceleration in

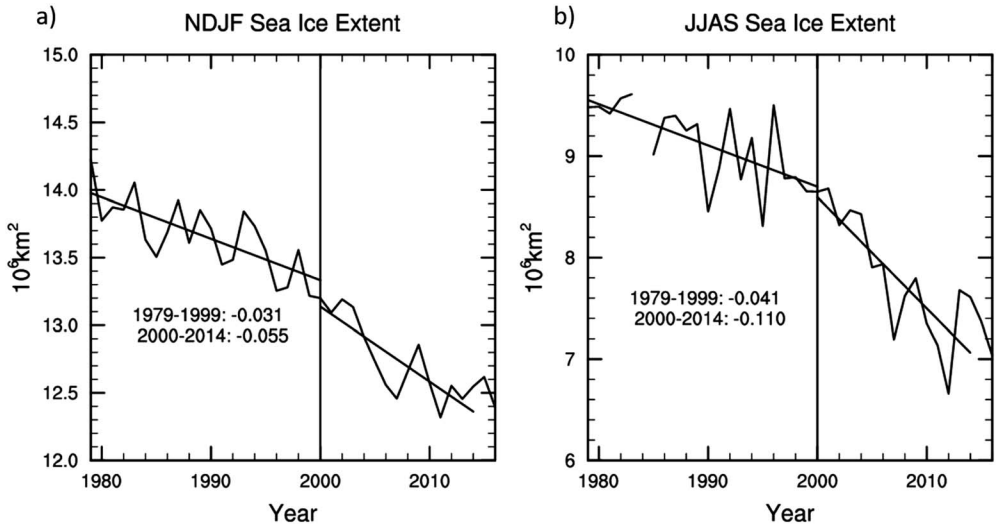

Figure 1. (a) Observed cold season (November-December-January-February) sea ice extent from 1979 through 2016 (10^6 km^2); linear trend calculated from 1979 to 1999 is $-0.031 \cdot 10^6$ km^2 yr^{-1}, and from 2000 to 2014 is $-0.055 \cdot 10^6$ km^2 yr^{-1}; (b) same as (a) except for warm season (June-July-August-September); linear trend calculated from 1979 to 1999 is $-0.041 \cdot 10^6$ km^2 yr^{-1}, and from 2000 to 2014 is $-0.110 \cdot 10^6$ km^2 yr^{-1}.

the rate of sea ice loss also has been noted by Comiso et al. (2008). Since the Interdecadal Pacific Oscillation in the tropical Pacific transitioned from positive to negative around 2000 (e.g., England et al., 2014; Kosaka & Xie, 2013; Meehl et al., 2016), and SSTs in the tropical Atlantic were warming during this time period (Meehl, Arblaster, et al., 2016), this suggests a possible linkage to decadal-time scale forcing via atmospheric teleconnections from the tropics to the Arctic. Such tropical forcing could have contributed to the rate of sea ice loss with associated ice albedo feedback and/or polar amplification on these time scales.

Patterns of atmospheric circulation trends in the Northern Hemisphere high latitudes were quite different pre- and post-2000 (Figures 2 and S1 in the supporting information). Sea level pressure (SLP) trends for NDJF 2000–2014 show an anomalous low in the North Atlantic, a high over eastern Europe and western Asia, and a significant anomalous high over the North Pacific. Figure S2 shows statistical significance for the observed SLP trends in Figures 2 and S1. Decreases in sea ice concentration occur north of Norway and Russia and north of the Bering Strait (Figure 2a). This is in contrast to the 1979–99 SLP and sea ice extent trends that show lower pressure extending from near Greenland across northern Asia and a weak anomalous high well to the south of the Aleutians in the Pacific (Figure S1a). For the JJAS season for 2000–2014, the observed SLP trends show a significant anomalous high covering almost the entire Arctic Ocean region with an anomalous low over the North Pacific and sea ice losses occurring north of Russia, Alaska, and Canada (Figure 2b). This can be compared to the 1979–1999 period where there is a weak anomalous high centered over Scandinavia and a faint anomalous low over northern Russia with most significant sea ice extent losses north of Alaska (Figure S1b). Thus, not only is the trend of area-averaged Arctic sea ice extent loss different between the two periods, but the atmospheric circulation patterns are considerably different as well.

We use an atmosphere-only model to test the hypothesis that forcing from anomalous tropical convective heating could drive different teleconnection patterns in different seasons over the high latitudes of the Northern Hemisphere. These patterns could then affect the rate of sea ice loss in different decadal epochs. The model is configured to run with specified climatological SSTs, forced by convective heating anomalies representing those observed in association with SST and precipitation anomalies in the 2000–2014 period in the tropical Pacific and Atlantic (following the methodology and the same experiments with the same model run by Meehl, Arblaster, et al., 2016). For the negative convective heating anomaly over the tropical Pacific representing conditions during the negative phase of the Interdecadal Pacific Oscillation from 2000 to 2014, there is a teleconnection pattern comparable to the observations for NDJF with an anomalous low in the North Atlantic, a high over eastern Europe and northwestern Asia, and a high over the North Pacific (Figure 2c). However, for the JJAS season, the SLP anomalies for this experiment (Figure 2d) are almost opposite to those observed (Figure 2b). The correspondence of many of the features in the observations and

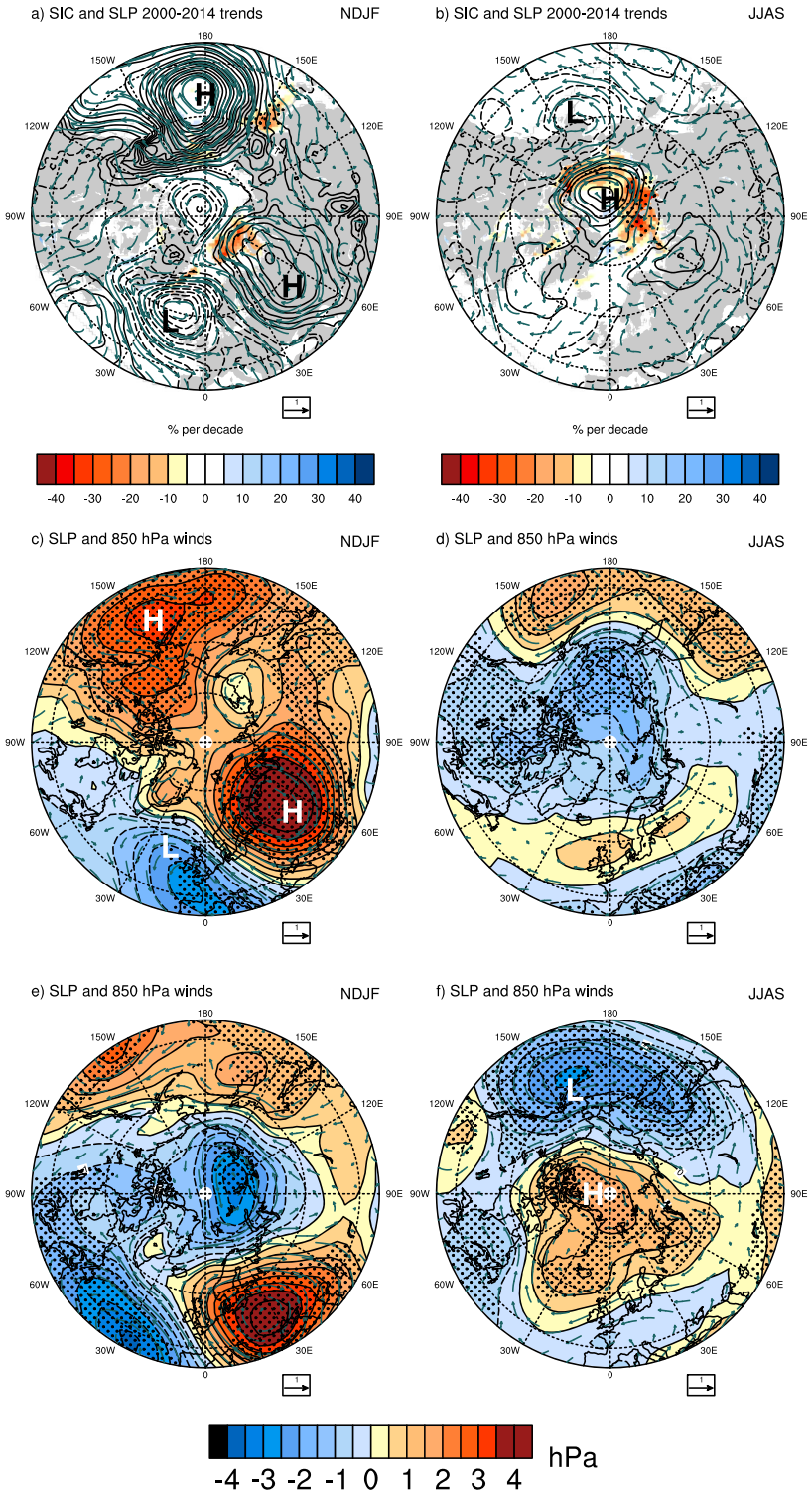

Figure 2. (a) November-December-January-February (NDJF) trend of sea ice concentration (colors, % decade^{-1}; stippling indicates significance at the 95% level), sea level pressure (SLP; hPa decade^{-1}, contours), and 850-hPa wind (vectors, m s^{-1} decade^{-1}, scaling arrow at lower right) from ERA-Interim reanalyses; (b) same as (a) except for June-July-August-September (JJAS); (c) atmospheric model with climatological sea surface temperatures and specified negative convective heating anomaly in the tropical Pacific centered at Eq, 135°W, SLP anomalies (hPa, contours, and colors; stippling denotes significance at the 95% level), and 850-hPa wind anomalies (m s^{-1}, scaling arrow at lower right) for 30-year NDJF average minus 100-year NDJF average from the control run; (d) same as (c) except for JJAS; (e) same as (c) except for positive convective heating anomaly in the tropical Atlantic at Eq, 30°W; (f) same as (e) except for JJAS. The "H" and "L" highlight a few relevant areas of correspondence between the model results and observations that are discussed in the text.

model simulation point to a likely contribution to the teleconnection pattern from the negative convective heating anomaly in the tropical Pacific, though there are some differences as well. In the model, the high over Eastern Europe is stronger than observed, while the high over the North Pacific is not quite as strong as observed. Additionally, the anomalous low over the Arctic Ocean in observations corresponds to minimum values of the anomalous highs over the North Pacific and Eastern Europe.

Meanwhile, for a positive convective heating anomaly placed over the tropical Atlantic, representing the positive SST and precipitation anomalies present there from 2000 to 2014, the model SLP anomaly pattern for NDJF (Figure 2e) is different from the observations (Figure 2a) However, for the JJAS season (Figure 2f), there is a much better correspondence to the observed pattern in Figure 2b, with a significant anomalous high over the Arctic, and an anomalous low over the North Pacific.

As could be expected from the SLP anomaly patterns, the surface warming trends from observations (Figure S3a) agree better in NDJF with the Pacific convective heating anomaly experiment with warming over the Arctic in NDJF (Figure S3c), but there is little agreement in JJAS (Figure S3d). But for the tropical Atlantic convective heating anomaly experiment, there is better agreement with the observations in JJAS (Figure S3b) with greatest warming over northern Canada and the Arctic Ocean (Figure S3f).

Wave activity flux (Takaya & Nakamura, 2001) at 200 hPa connects Rossby wave sources from tropical convective heating anomalies to extratropical teleconnection patterns (Figure S4). For the JJAS warm season, wave activity flux from the positive convective heating anomaly in the tropical Atlantic is associated with negative stream function anomalies in the subtropical jet over the Mediterranean region, with some wave energy affecting the positive stream function anomalies near Iceland (Figure S4a). Wave activity flux continues eastward along the jet waveguide with negative stream function anomalies across Asia and the Pacific. The easterly stream function anomalies on the northern flanks of these negative anomalies then correspond to positive stream function anomalies over much of the Arctic associated with the positive SLP anomalies there (Figure 2f). For the NDJF cold season, the negative convective heating anomaly in the equatorial eastern Pacific drives wave activity flux northeastward to the wave train setup over North America and the North Atlantic, which extends to a positive stream function anomaly over Scandinavia (Figure S4b). These 200-hPa stream function anomalies have corresponding surface counterparts in the SLP anomalies in Figure 2c, thus providing evidence of the Rossby wave response mechanism that has previously been documented in the literature (e.g., Takaya & Nakamura, 2001).

To better quantify the connection between changes in sea ice concentration, surface winds, and ice drift, areas are defined where seasonal sea ice shows decreasing trends in the 2000–2014 period in Figures 2a and 2b: Bering area NDJF: 170°W–170°E, 70–75°N, and JJAS: 120°W–170°E, 70–75°N; European area NDJF: 30°E–70°E, 75°N–80°N, and JJAS: 30°E–150°E, 75°N–85°N. The pattern of large amplitude ice drift trends in the 2000–2014 period (Figure 3) corresponds to the areas of larger amplitude surface wind trends (Figures 2a and 2b) in both seasons. Meanwhile, the larger amplitude SLP teleconnection patterns and thus stronger surface winds in the 2000–2014 period compared to 1979–1999 (about a factor of three larger in NDJF, Figures 4a and 4b, and almost a factor of 10 larger in JJAS, Figures 4e and 4f) are associated with increases in ice drift velocities of that relative magnitude (Figures 4c, 4d, 4g, and 4h). There is even a large and significant reversal of ice drift trend direction in the European sector in NDJF 2000–2014 (Figure 4d) compared to NDJF 1979–1999 (Figure 4c) amounting to a net change of nearly 1 cm s^{-1} $decade^{-1}$.

The European and Bering areas have the largest trends of decreasing sea ice concentration in the 2000–2014 period compared to 1979–1999. The decreasing sea ice concentration trends in the latter period are greater by factors of about 2 to nearly 10 (Figures 4i, 4j, 4m, and 4n). Trends in total sea ice extent were shown in Figure 1, while sea ice concentration is a more meaningful metric for area averages in Figure 4 for comparison to other area-averaged quantities like surface heat flux. In these regions, the anomalously strong westerly surface wind trends in NDJF 2000–2014 (Figure 4b) associated with the anomalous highs over the European and Bering Strait sectors (Figure 2a) force anomalously strong westerly ice drifts (Figure 4d). The combination of anomalous wind and ice drift, while important for the changes in sea ice concentration, are not the only factors at work. For example, the wind and drift speed changes (from 1979–1999 to 2000–2014) are highest in the Bering sector for the NDJF period and yet the NDJF sea ice concentration changes are strongest for the European sector. Yet the previously established connection between strong surface winds and ice drifts (Spreen et al., 2011) is typically associated with reduced multiyear ice (Kwok et al., 2013) and is seen here

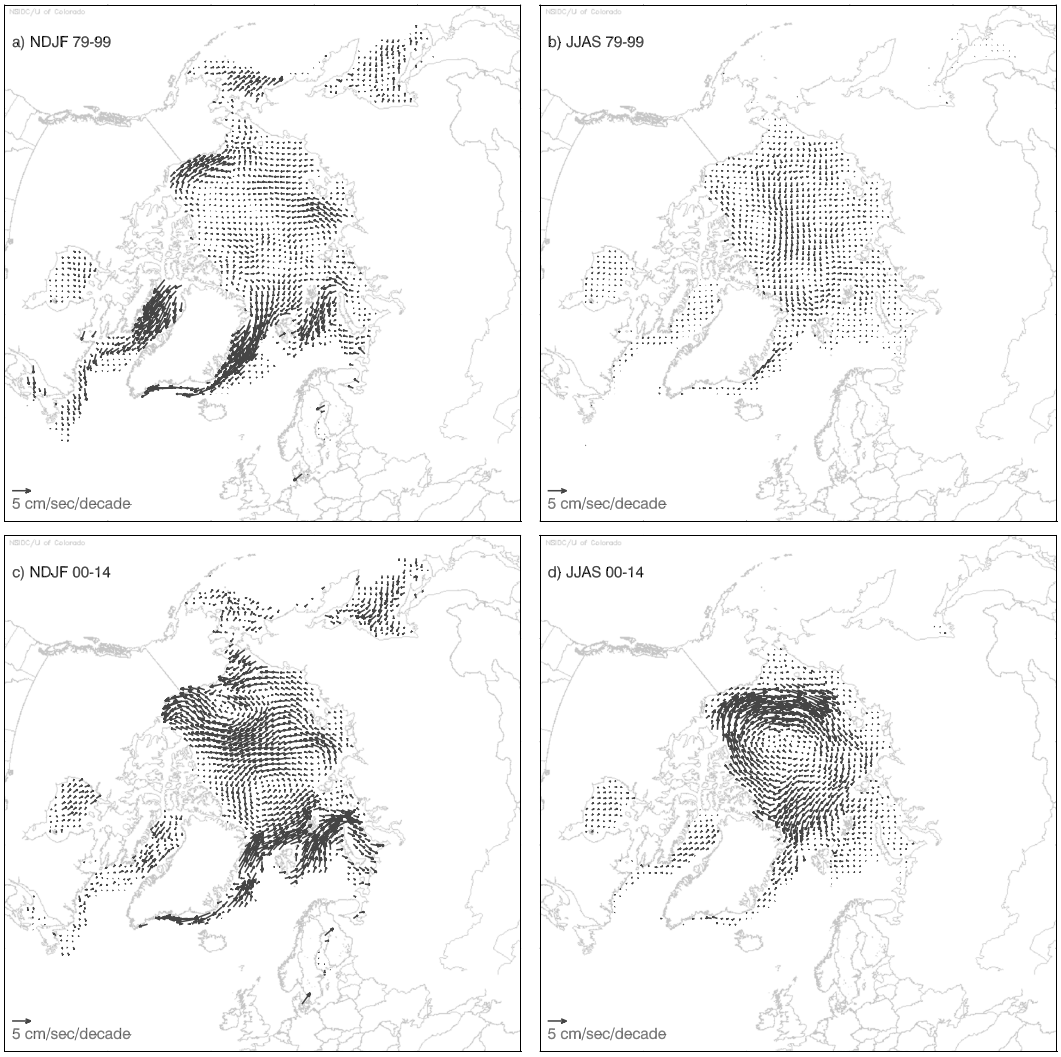

Figure 3. Ice drift trends (cm s^{-1} $decade^{-1}$), (a) November-December-January-February (NDFJ) 1979–1999, (b) June-July-August-September (JJAS) 1979–1999, (c) NDJF 2000–2014, and (d) JJAS 2000–2014; 5 cm s^{-1} $decade^{-1}$ scaling vector at lower left in each panel.

to produce accelerated trends for sea ice concentration loss (Figure 4j). Similar processes occur in JJAS (Figures 4f, 4h, and 4n).

Net surface heat flux then follows these changes in sea ice concentration that are driven mainly by anomalous winds and ice drift, with thinner and weaker sea ice (after around 2000) being more responsive to the stronger wind forcing (Kwok et al., 2013). The NDJF 2000–2014 period shows large negative net surface heat flux trends. These range from about -7 W m^{-2} $decade^{-1}$ in the Bering sector (Figure 4k, negative sign indicates upward heat flux, as leads and open areas show up in the thinner sea ice, and heat is removed from the ocean surface in the dark, cold Arctic winter) to over -20 W m^{-2} $decade^{-1}$ in the European sector (Figure 4l). However, the complicated nature of process interactions can be illustrated by an increase in low clouds by over 5% $decade^{-1}$ in the Bering sector and a decrease of about 4% $decade^{-1}$ in the European sector.

For JJAS, there are increases in net surface heat flux of about +10 W m^{-2} $decade^{-1}$ (downward heat flux into the surface) in both the Bering and European sectors (Figures 4o and 4p). This is associated with the anomalous high SLP trends over the Arctic, stronger surface winds and ice drifts, reduced sea ice concentration, and increased absorbed solar at the surface due to less sea ice as an indication of ice-albedo feedback. Consequently, there are significant increases in downward shortwave of nearly +13 W m^{-2} $decade^{-1}$ in the Bering sector, and about +6 W m^{-2} $decade^{-1}$ in the European sector with little change in low clouds.

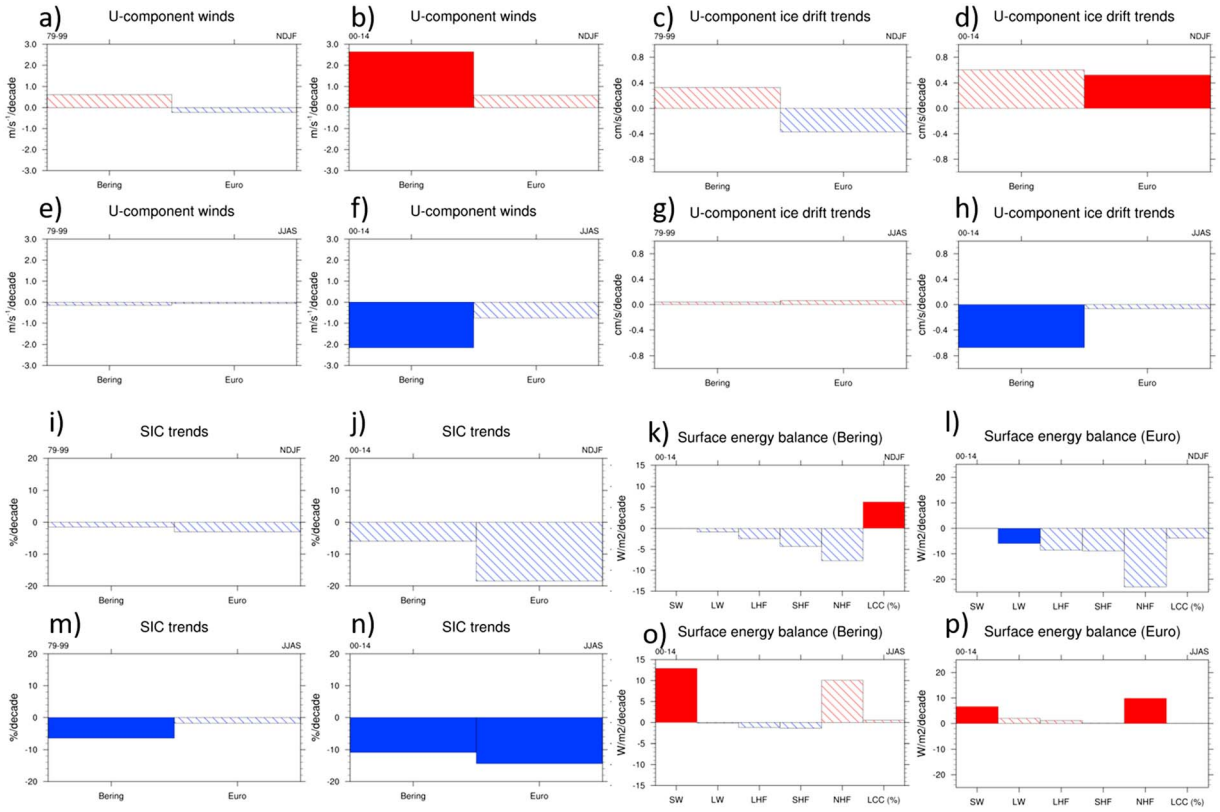

Figure 4. Linear trends for Bering and European sectors in the Arctic (areas denoted in the text; the solid bars denote 95% significance), (a) *u* component surface wind trends (m s^{-1} $decade^{-1}$), November-December-January-February (NDJF) 1979–99; (b) same as (a) except for 2000–2014; (c) same as (a) except for ice drift trends (cm s^{-1} $decade^{-1}$); (d) same as (c) except for 2000–2014; (e) same as (a) except for June-July-August-September (JJAS); (f) same as (b) except for JJAS; (g) same as (c) except for JJAS; (h) same as (d) except for JJAS; (i) same as (a) except for sea ice concentration trends (% $decade^{-1}$); (j) same as (i) except for 2000–2014; (k) surface energy balance trends for Bering sector only, NDJF (W m^{-2} $decade^{-1}$), positive sign denotes energy into the surface, SW = shortwave, LW = longwave, LHF = latent heat flux, SHF = sensible heat flux, NHF = net heat flux; bar at far right (LCC) is low cloud trends (% $decade^{-1}$); (l) same as (k) except for European sector; (m) same as (i) except for JJAS; (n) same as (j) except for JJAS; (o) same as (k) except for JJAS; (p) same as (l) except for JJAS.

These results also indicate that, as in the cold season, the net surface heat flux is reacting to the underlying sea ice conditions. This suggests that increased wind forcing and accelerated ice drift in the cold season (Kwok et al., 2013; Spreen et al., 2011) are likely causing changes in sea ice concentration to which the heat flux then reacts. This is supported by trends in surface heat convergence (Figure S5). These show positive heat convergence trends ranging from about $+0.5 \times 10^{-5}$ K s^{-1} $decade^{-1}$ to $+0.3 \times 10^{-5}$ K s^{-1} $decade^{-1}$ in the two time periods for NDJF (zonally averaged values over ocean grid points from 70–85°N). Net heat convergence trends in JJAS are +0.3 W m^{-2} $decade^{-1}$ in the first period and about -0.2 W m^{-2} $decade^{-1}$ in the more recent period. This is related to the anomalous circulation over the Arctic that is in the same sense in NDFJ between the two periods (with anomalous negative trend values in both periods) and nearly opposite in JJAS (with mostly negative trend values over the Arctic in 1979–1999 and positive in 2000–2014). This again indicates that the main drivers are atmospheric circulation patterns and associated surface winds. Ice drifts respond to those winds that act to weaken and thin the ice and reduce concentrations.

These results can be summarized in Figure 5 where the accelerated rate of decrease in Arctic sea ice extent after around 2000 is shown to have a contribution from decadal changes in tropical SSTs, associated precipitation and convective heating anomalies, and seasonally dependent teleconnections over the Arctic. The consequent stronger surface winds and ice drifts are then associated with decreases in sea ice concentration, and the surface heat flux responds to those seasonal changes in sea ice concentration. Thus, there are notable contributions to the accelerated decrease in Arctic sea ice concentration from 2000 to 2014 involving atmospheric teleconnections emanating from variations in decadal changes in tropical SSTs and precipitation/convective heating anomalies.

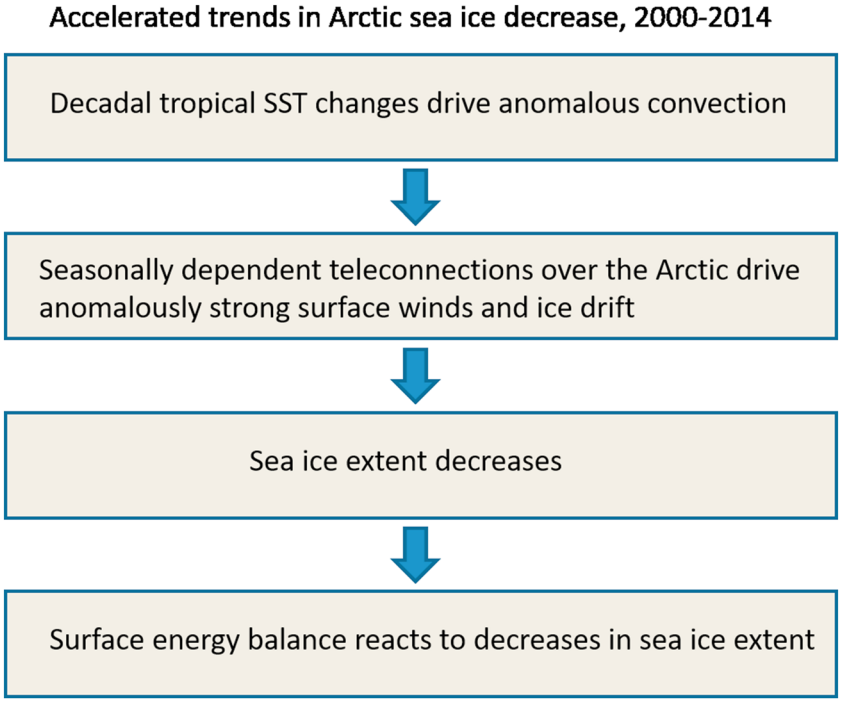

Figure 5. Schematic of the processes linking tropical decadal variability and accelerated trend reductions in Arctic sea ice extent from 2000 to 2014.

Of course, in the climate system, there is always more than one thing going on in addition to internally generated variability. These include, but are not limited to, increases of GHGs, changes in aerosols, and so on. The tropical convective heat sources and associated teleconnections arising from decadal SST changes that are, presumably, mostly internally generated, are just one set of processes in the climate system that can *contribute*, along with other factors, to trends in Arctic sea ice concentration.

Data availability

Sea ice extent from 1979 through 2016 (10^6 km^2) precalculated monthly extent values from the .csv files in version 3 available from ftp://sidads.colorado.edu/DATASETS/NOAA/G02135/ that are qualitatively comparable to the quality controlled files that end in February 2017.

The SLP, surface energy balance, and U-winds are from ERA-Interim (Dee et al., 2011) available from https://www.ecmwf.int/en/forecasts/datasets/archive-datasets/reanalysis-datasets/era-interim. Sea ice drift data (Tschudi et al., 2016) available from http://nsidc.org/data/NSIDC-0116 and accessed 27 June 2018. Sea ice concentration data (Cavalieri et al., 1996) available from http://nsidc.org/data/NSIDC-0051, accessed 27 March 2017. The model experiments are from Meehl, Arblaster, et al. (2016).

Acknowledgments
The authors acknowledge Haiyan Teng for her consultations on the wave activity flux calculations. Portions of this study were supported by the Regional and Global Model Analysis Program (RGMA) of the U.S. Department of Energy's Office of Biological & Environmental Research (BER) Cooperative Agreement DE-FC02-97ER62402 and the National Science Foundation. The National Center for Atmospheric Research is sponsored by the National Science Foundation. This work also was supported by the Australian Research Council Centre of Excellence for Climate Extremes (grant CE170100023).

References

Cavalieri, D. J., Parkinson, C. L., Gloersen, P., & Zwally, H. J. (1996). updated yearly. Sea ice concentrations from Nimbus-7 SMMR and DMSP SSM/I-SSMIS passive microwave data, version 1. January 1979 to December 2015. Boulder, Colorado USA. NASA National Snow and Ice Data Center Distributed Active Archive Center. https://doi.org/10.5067/8GQ8LZQVL0VL

Cohen, J., Pfeiffer, K., & Francis, J. A. (2018). Warm Arctic episodes linked with increased frequency of extreme winter weather in the United States. *Nature Communications*, *9*, 869. https://doi.org/10.1038/s41467-018-02992-9

Comiso, J. C., Parkinson, C. L., Gersten, R., & Stock, L. (2008). Accelerated decline in the Arctic sea ice cover. *Geophysical Research Letters*, *35*, L01703. https://doi.org/10.1029/2007GL031972

Cvijanovic, I., Santer, B. D., Bonfils, C., Lucas, D. D., Chiang, J. C. H., & Zimmerman, S. (2017). Future loss of Arctic sea-ice cover could drive a substantial decrease in California's rainfall. *Nature Communications*, *8*, 1947. https://doi.org/10.1038/s41467-017-4

Dee, D. P., Uppala, S., Simmons, A., Berrisford, P., Poli, P., Kobayashi, S., et al. (2011). The ERA-Interim reanalysis: Configuration and performance of the data assimilation system. *Quarterly Journal of the Royal Meteorological Society*, *137*, 553–597. https://doi.org/10.1002/qj.828

Ding, Q., Wallace, J. M., Battisti, D. S., Steig, E. J., Gallant, A. J. E., & Kim, H.-J. (2014). Tropical forcing of the recent rapid Arctic warming in northeastern Canada and Greenland. *Nature*, *509*. https://doi.org/10.1038/nature13260

England, M. H., McGregor, S., Spence, P., Meehl, G. A., Timmermann, A., & Cai, W. (2014). Slowdown of surface greenhouse warming due to recent Pacific trade wind acceleration. *Nature Climate Change*, *4*, 222–227.

Kosaka, Y., & Xie, S.-P. (2013). Recent global-warming hiatus tied to equatorial Pacific surface cooling. *Nature*, *501*(7467), 403–407. https://doi.org/10.1038/nature12534

Kwok, R., Spreen, G., & Pang, S. (2013). Arctic sea ice circulation and drift speed: Decadal trends and ocean currents. *Journal of Geophysical Research: Oceans*, *118*, 2408–2425. https://doi.org/10.1002/jgrc.20191

Lee, S., Gong, T., Johnson, N., Feldstein, S. B., & Pollard, D. (2011). On the possible link between tropical convection and the Northern Hemisphere Arctic surface air temperature change between 1958 and 2001. *Journal of Climate*, *24*(16), 4350–4367. https://doi.org/10.1175/2011JCLI4003.1

Li, X., Holland, D. M., Gerber, E. P., & Yoo, C. (2014). Impacts of the north and tropical Atlantic Ocean on the Antarctic Peninsula and sea ice. *Nature*, *505*(7484), 538–542. https://doi.org/10.1038/nature12945

Meehl, G. A., Arblaster, J. M., Bitz, C. M., Chung, C. T. Y., & Teng, H. (2016). Antarctic sea-ice expansion between 2000 and 2014 driven by tropical Pacific decadal climate variability. *Nature Geoscience*, *9*(8), 590–595. https://doi.org/10.1038/NGEO2751

Meehl, G. A., Hu, A., & Teng, H. (2016). Initialized decadal prediction for transition to positive phase of the Interdecadal Pacific Oscillation. *Nature Communications*, *7*. https://doi.org/10.1038/NCOMMS11718

Purich, A., England, M. H., Cai, W., Chikamoto, Y., Timmermann, A., & Fyfe, J. C. (2016). Tropical Pacific SST drivers of recent Antarctic sea ice trends. *Journal of Climate*, *29*(24), 8931–8948. https://doi.org/10.1175/JCLI-D-16-0440.1

Screen, J. A., Deser, C., Smith, D. M., Zhang, X., Blackport, R., Kushner, P. J., et al. (2018). Consistency and discrepancy in the atmospheric response to Arctic sea-ice loss across climate models. *Nature Geoscience*, *11*, 155–163. https://doi.org/10.1038/s41561-018-0059-y

Spreen, G., Kwok, R., & Menemenlis, D. (2011). Trends in Arctic sea ice drift and the role of wind forcing: 1992–2009. *Geophysical Research Letters*, *38*, L19501. https://doi.org/10.1029/2011GL048970

Takaya, K., & Nakamura, H. (2001). A formulation of a phase-independent wave-activity flux for stationary and migratory quasigeostrophic eddies on a zonally varying basic flow. *Journal of the Atmospheric Sciences*, *58*(6), 608–627. https://doi.org/10.1175/1520-0469(2001)058<0608:AFOAPI>2.0.CO;2

Tschudi, M., Fowler, C., Maslanik, J., Stewart, J. S., & Meier, W. (2016). Polar Pathfinder Daily 25 km EASE-Grid Sea Ice Motion Vectors, Version 3. January 1979 to December 2015. Boulder, Colorado USA. NASA National Snow and Ice Data Center Distributed Active Archive Center. https://doi.org/10.5067/O57VAIT2AYYY